Available online at www.sciencedirect.com
ScienceDirect
Journal of Organometallic Chemistry 693 (2008) 492–504
Journal of Organometallic Chemistry
www.elsevier.com/locate/jorganchem

Triphenyl lead, tin and germanium coordination compounds derived from 9H-3-thia-1,4a,9-triaza-fluorene-2,4-dithione

Adrián Peña-Hueso, Adriana Esparza-Ruiz, Iris Ramos-García, Angelina Flores-Parra *, Rosalinda Contreras *

Departamento de Química, Cinvestav, A.P. 14-740, CP 07000 México, D.F., Mexico

Received 9 November 2007; accepted 12 November 2007
Available online 3 January 2008

Abstract

Reactions of potassium 4-thioxo-3-thia-1,4a,9-triaza-fluorene-2-thiolate with Ph_3PbCl, Ph_3SnCl and Ph_3GeCl provided the corresponding metal pentacoordinated compounds **2**–**4**. Addition of THF afforded their hexacoordinated derivatives (**5**–**7**). Adducts of **2** and **3** with DMSO (**8**, **10**), pyridine (**9**, **11**), Ph_3PO (**12**, **14**) CH_3OH (**13**, **15**), respectively were synthesized. Compound **2** afforded the H_2O adduct (**16**). In all cases the metal atom is chelated by the ligand through a covalent bond with S2 and a coordination bond with N1 forming four membered rings. Compounds were identified by ^{1}H, ^{13}C, ^{15}N, ^{119}Sn and ^{207}Pb. X-ray diffraction structures of **2**, **3**, **8**, **9**, **11**, **14** and **16** were obtained.

Keywords: Organogermanium; Organotin; Organolead; 9H-3-thia-1,4a,9-triaza-fluorene-2,4-dithione; ^{207}Pb NMR; ^{119}Sn NMR

1. Introduction

We are currently investigating the chemistry of organometallic compounds of the group 14 elements [1,2] and particularly those coordinated to planar and aromatic molecules [3–8]. These ligands and the metal atoms provide hypervalent metal atoms and versatile coordination modes. Their rigid structures make them suitable models for the study of weak interactions in the solid-state. Interest in these coordination compounds is also based on the use of multinuclear magnetic resonance techniques for their analyses in solution.

The heavier elements of group 14 show rich coordination chemistry [9–12]. In addition tin compounds have applications in industry, agriculture and medicine [13–17], whereas the relevance of lead coordination compounds is based on their application in pharmacology and toxicology [18,19]. Of additional interest in lead and tin coordination compounds is the search for new ligands which could be useful in detoxification therapies [20,21]. Germanium has wide applications for fabrication of electronic components [22], as chemotherapeutic agents of low mammalian toxicity [23,24] and as radioprotective agents [25].

Compounds derived from benzimidazole have diverse biocidales activities and pharmaceutical applications [26–28]. In particular tricyclic benzimidazole derivatives have been investigated as potential inhibitors of dihydrofolate reductase in the search for anticancer and antibacterial agents [29–31] and for DNA intercalating agents [31].

2. Results and discussion

Herein, we report the syntheses and characterization of coordination compounds of triphenyl lead, tin, and germanium with the new aromatic tetracyclic ligand: 9H-3-thia-1,4a,9-triaza-fluorene-2,4-dithione **1a**, Scheme 1.

The interest of a detailed structural analysis of the metal coordination compounds derived from **1a** is due to the fact

* Corresponding authors. Tel.: +55 5061 3720; fax: +55 5061 3389 (A. Flores-Parra).
E-mail address: aflores@cinvestav.mx (A. Flores-Parra).

0022-328X/$ - see front matter © 2007 Elsevier B.V. All rights reserved.
doi:10.1016/j.jorganchem.2007.11.040

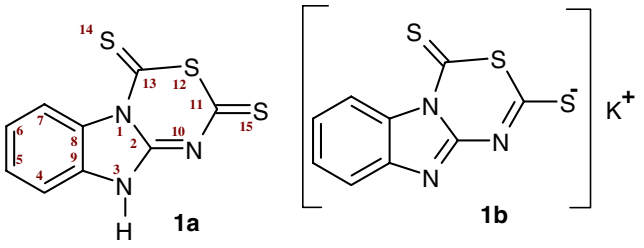

Scheme 1. Structure of the 9H-3-thia-1,4a,9-triaza-fluorene-2,4-dithione **1a**.

that a bidentate coordination of ligand to metal atoms could occur in at least five different ways, see Scheme 2.

The potassium thiolate (**1b**) is the precursor of compound **1a**. Thiolate **1b** is an aromatic tricyclic molecule prepared from 2-aminobenzimidazole, CS_2 and KOH in DMF, it is a stable bright yellow solid, soluble in polar solvents. The simple one-step synthesis of **1b**, contrast with the reported multistep and complex synthesis of a similar compound derived from imidazole [32].

Reactions of potassium 4-thioxo-3-thia-1,4a,9-triaza-fluorene-2-thiolate (**1b**) with Ph_3PbCl, Ph_3SnCl and Ph_3GeCl provided the corresponding metal pentacoordinated compounds **2**–**4**, Scheme 3. Addition of THF afforded their hexacoordinated derivatives (**5**–**7**). Adducts of **2** and **3** with DMSO (**8**, **10**), pyridine (**9**, **11**), Ph_3PO (**12**, **14**) CH_3OH (**13**, **15**), respectively were synthesized. Compound **2** gave the H_2O adduct (**16**).

2.1. NMR studies

Compound **1a** and the potassium thiolate **1b** were characterized by NMR. The assignment of the ^1H and ^{13}C signals of **1b** was based on COLOC, HETCOR and COSY

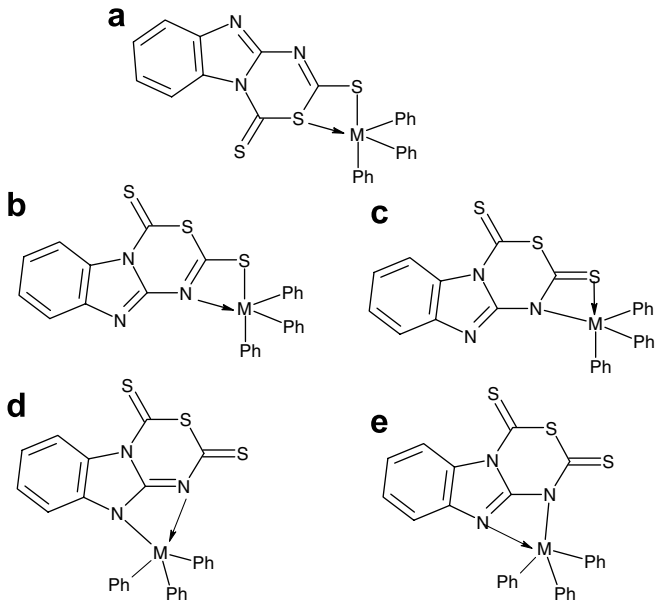

Scheme 2. Five possible coordination modes of a triphenylmetal fragment to ligand **1**.

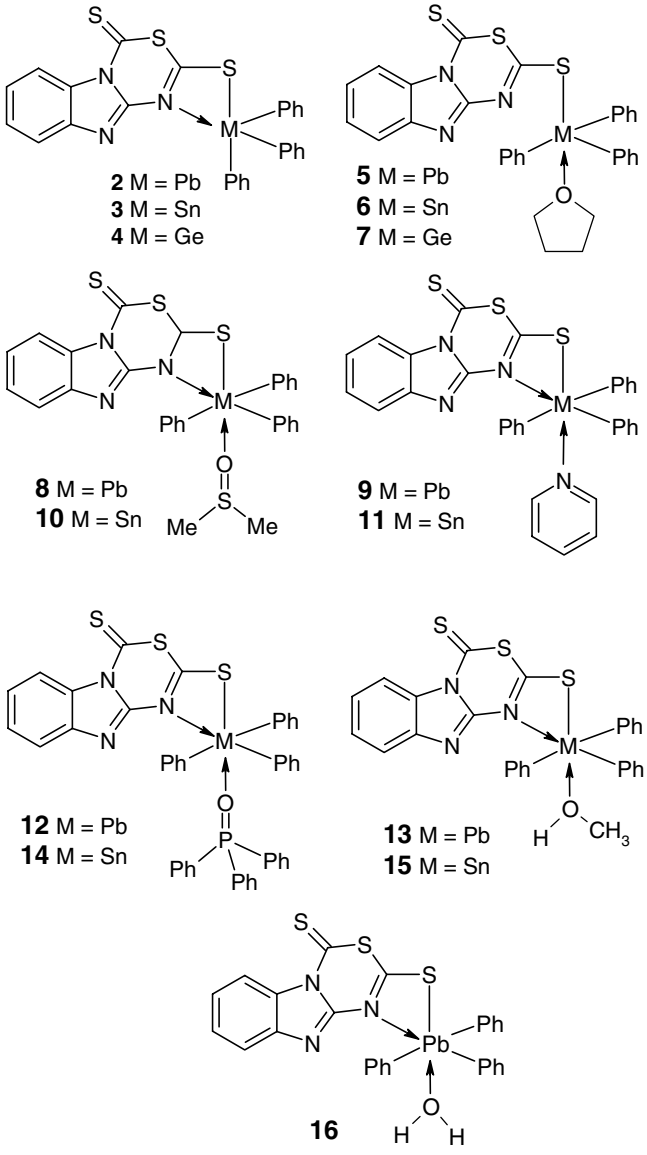

Scheme 3.

experiments, Table 1. The structure of compound **1b** was also deduced from the ^{15}N data (N1, $\delta = -191.4$; N3, $\delta = -157.4$; and N10, $\delta = -136.3$ ppm) [33]. For compound **1b**, the ^1H signal of H7 is found at higher frequencies than the starting material due to the proximity of S14; a similar effect in H4 is due to the presence of the N-lone pair at N3, Scheme 1 and Table 1. The ^{13}C spectrum shows nine signals, two to higher frequencies that belong to the sulfur *ipso* carbons. The one found at $\delta = 194.1$ ppm corresponds to the thione carbon atom, whereas the signal of C11 ($\delta = 184.4$ ppm) base of a thiolate group, indicates that the charge is located at S15. Carbon atoms C8 and C9 have different chemical shifts, the one adjacent to the N3 with a lone pair appears at $\delta = 143.7$ ppm, whereas C8 close to a substituted nitrogen atom gives a signal at $\delta = 130.9$ ppm, [34]. Compound **1a** has a proton located at N3, as is deduced from the ^{13}C signal of C9 which appears at $\delta = 129.3$ ppm, and the C11 (193.0 ppm) and

Table 1
NMR ^{1}H and ^{13}C data of compounds **1**, **1a**, **2**, **3**, **8**–**11**

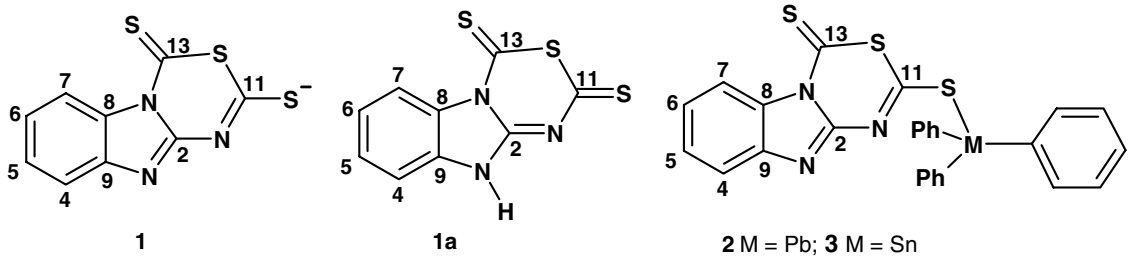

	2	4	5	6	7	8	9	11	13	*i*	*o*	*m*	*p*
1 (DMSO-d_6)	150.5	118.1 7.55	126.8 7.40	122.3 7.22	117.3 8.92	130.9	143.7	184.4	194.1				
1a (DMSO-d_6)	148.3	113.6 7.53	125.2 7.39	129.0 7.55	118.3 8.95	131.2	129.3	193.0	194.8				
2 ($CDCl_3$)	147.6	120.0 7.87	127.4 7.59	124.9 7.50	117.8 8.99	131.0	142.8	176.0	185.9	155.6	137.4 7.98	130.5 7.55	129.9 7.40
8 (DMSO-d_6)	150.0	118.2 7.59	126.9 7.41	122.6 7.23	117.3 8.92	131.3	143.4	183.2	193.2	159.5	136.2 7.88	130.5 7.64	130.1 7.46
9 (Py-d_5)	149.7	118.8 7.53	126.8 7.10	123.3 6.93	117.7 8.72	131.2	143.4	181.0	190.0	158.8	137.1 7.96	130.2 7.22	129.5 7.00
3 ($CDCl_3$)	147.7	118.7 7.78	126.9 7.51	124.0 7.40	117.4 9.01	130.8	141.9	178.3	187.0	139.0	136.9 8.04	128.5 7.45	129.5 7.42
10 (DMSO-d_6)	150.8	118.2 7.63	126.6 7.43	122.3 7.25	117.5 9.09	131.6	143.7	185.1	193.4	143.7	136.6 8.03	128.4 7.48	129.0 7.46
11 (Py-d_5)	150.6	118.0 7.78	127.0 7.41	123.1 7.24	118.0 9.15	131.7	143.9	183.7	192.5	143.9	137.1 8.04	130.3 7.51	129.6 7.49
13 CD_3OD		117.7/7.55 7.55	126.9/7.41 7.41	122.9/7.24 7.24	117.7/9.00 9.00	131.0	142.8	186.0			136.5 7.89	130.0 7.55	129.2 7.40
15 CD_3OD	151.2	117.6/7.56 7.56	126.9/7.41 7.41	122.9/7.25 7.25	117.7/9.02 9.02	131.4	142.6	188.6	193.5	141.7	136.3 7.85	128.7 7.47	129.5 7.45

C13 (194.1 ppm) chemical shifts which correspond to thione groups.

The reaction of compound **1b** with triphenylmetal chlorides (lead, tin and germanium) afforded the corresponding pentacoordinated compounds **2**–**4**, Scheme 3. The lead compound **2** and its derivatives are very stable, whereas the tin compounds were hydrolyzed in the presence of moisture and the germanium compound **4** was decomposed by the addition of Lewis bases even in anhydrous conditions. Compounds **2** and **3** were characterized by NMR in $CDCl_3$, solvent in which **4** was insoluble, Tables 1–3. Comparison of the ^{13}C data of compounds **2** and **3** with those of the neutral ligand **1a** indicated that the metal is bonded to S15, and it is assumed that the nitrogen is coordinated to the metal atom, as has been observed for heterocycles thionates and diverse metal atoms [35]. The resonances of ^{207}Pb of compound **2** ($\delta = -3.1$ ppm) and the ^{119}Sn of compound **3** ($\delta = -75.6$ ppm) are characteristic of tetracoordinated metal atoms, indicating that the nitrogen coordination is weak and has little effect on their chemical shifts [36–41]. The X-ray diffraction of compounds **2** and **3** confirmed the nitrogen coordination as we will discuss later. The high resolution mass spectra, is in agreement with one ligand linked to the MPh_3 fragment.

Table 2
NMR ^{207}Pb and ^{119}Sn data

Solvent		^{207}Pb		^{119}Sn
$CDCl_3$	**2**	−3.1	**3**	−75.6
THF-d_8	**5**	−104.9	**6**	−125.5
DMSO-d_6	**8**	−199.4	**10**	−226.1
Py-d_5	**9**	−217.2	**11**	−231.8
THF-d_8	**12**	−214.5	**14**	−251.0
CD_3OH	**13**	−136.1	**15**	−180.2

Solution of **2**–**4** in THF produced the hexacoordinated derivatives **5**–**7** as is deduced from the NMR data, Table 4. The ^{13}C NMR data (in THF-d_8) indicate that compounds **5**–**7** have similar structures. The ^{119}Sn and ^{207}Pb spectra of compounds **5** and **6** showed an important shift to lower frequencies with respect to compounds **2** and **3** in $CDCl_3$, attributed to the THF coordination, Table 2.

The ^{207}Pb spectrum of compound **2** in DMSO-d_6 gives a signal at $\delta = -199.4$ ppm characteristic of DMSO coordination and attributed to compound **8**, Tables 2 and 3. The ^{207}Pb spectrum of **2** in pyridine-d_6 gave a resonance at $\delta = -217.2$ ppm assigned to the hexacoordinated pyridine complex **9**. In both cases the ^{207}Pb signals were shifted to lower frequencies by 196.3 and 214.1 ppm.

Table 3
Values of observed coupling constants $^{n}J(^{13}C–^{119}Sn)$ or $^{n}J(^{13}C–^{207}Pb)$ for M–Ph groups

	2	3	5	6	8	10	9	11	13
i			633.7						
o	84.6	46.1	82.1	44.5	87.1	46.7	78.4	43.6	47.4
m		51.4	130.1	64.6		70.6	110.1		70.0
p	22.3	13.1				15.6			14.6

Table 4
^{1}H and ^{13}C NMR data of compounds **5**–**7** (THF-d_8)

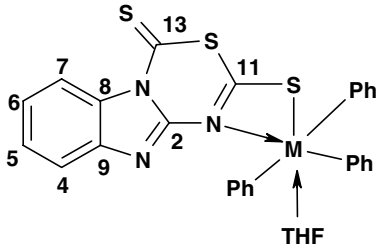

5 M = Pb; **6** M = Sn; **7** M = Ge

C atom	5	6	7
2	149.6	148.7	148.6
4	120.2/7.78	120.4/7.75	123.4/7.59
5	127.8/7.63	127.9/7.44	128.6/7.46
6	124.8/7.48	125.2/7.33	127.5/7.41
7	118.6/9.03	118.4/8.93	117.5/9.04
8	132.3	132.0	130.5
9	144.5	143.8	137.8
11	179.6	176.9	183.2
13	189.6	187.6	193.2
i	159.2	140.4	137.5
o	138.5/8.15	138.0/8.01	134.3/7.59
m	130.9/7.54	129.6/7.39	128.0/7.39
p	130.3/7.38	130.5/7.36	129.4/7.21

When tin compound **3** was dissolved in DMSO, compound **10** was formed (^{119}Sn $\delta = -226.1$ ppm), while the solution in pyridine gave compound **11** (^{119}Sn $\delta = -231.8$ ppm). From the NMR tubes, crystals of **8**, **9** and **11** were obtained which were characterized by X-ray diffraction.

When compounds **2** and **3** were dissolved in THF and an excess of Ph_3PO added, the corresponding adducts **12** and **14** were obtained (^{207}Pb $\delta = -214.5$ and ^{119}Sn $\delta = -251.0$ ppm), Table 2. Compound **12** was only characterized in solution, whereas **14** was analyzed by X-ray diffraction.

The solution of compound **2** in methanol presents a ^{207}Pb resonance at $\delta = -136.1$ ppm, attributed to complex **13** whereas the ^{119}Sn spectrum of the corresponding methanol complex of **3**, appears at $\delta = -180.2$ ppm (**15**), Table 2. From the NMR tube of compound **13**, a few crystals of one molecule of **2** together with its water complex (**16**) were obtained. Attempts to obtain compound **16** by adding water to **2** previously dissolved in $CHCl_3$ were unsuccessful. An analogous tin water adduct from compound **3** was not obtained due to its hydrolysis.

2.2. X-ray diffraction analyses

The X-ray diffraction analyses were performed for compounds **2**, **3**, **8**, **9**, **11**, **14** and **16**. In all structures, the ligand is bidentated, bonded to the metal through S15 and N10. The confirmation of the nitrogen coordination to the metal atom is based on the nitrogen–metal atom distance which is shorter than the sum of the van der Waals radii and on the orientation of the plane of the tricyclic fragment of the molecule that allows the approach of the nitrogen lone pair to the metal atom. In molecules lacking a nitrogen atom in *ortho* position to a thiophenol, the ring plane is not aligned with the S–M bond, as for example, in the solid state structures of thiophenoltriphenyl lead [42] and thionaphtoltriphenyl tin [43]. The coordination forms four membered rings M–S–C–N with penta- and hexacoordinated triorganyl tin or lead compounds. Some examples of these chelates for tin [44–46] and lead [47,48] are known. Selected bond lengths and angles are in Table 5, and crystal data and structure refinement in Tables 6 and 7.

Compound **2** has two molecules in the asymmetric unit. The lead atoms are hexacoordinated, with four covalent bonds and are coordinated intramolecularly to N {N10 → Pb16 = 3.093(7), N50 → Pb56 = 3.162(7) Å, $\sum_{vwr} = 3.90$ Å [49]} and to the S54 of another molecule, forming a polymer {Pb16···S54 3.607(3), Pb56···S14 3.497(3) Å, $\sum_{vwr} = 4.1$ Å [49]}, with the cooperation of S12 and S52 π-interaction with one of the Pb-phenyl groups [distances of S to ring centroids 3.485(5) and 3.460(5) Å], Fig. 1. The metal atoms do not have an ideal octahedral geometry. A distortion is originated by the angular tension of the four membered ring (C–S–M–N). The angles N10–Pb16–C23 and N50–Pb56–C63 are 149.6(3)° and 147.5(3)°, respectively. The two sulfur atoms are *trans*, with angles S15–Pb16–S54 173.60(7)° and S14–Pb56–S55 173.37(8)°. An intermolecular π-stacking occurs between the two aromatic tricycles [distances between centroids: 3.620(5) and 3.636(5) Å], Fig. 2 [50].

Compound **3** has a pentacoordinated tin atom where the fifth bond is the N10–Sn coordination bond {3.088(3) Å, $\sum_{vwr} = 3.9$ Å, [49]}, Fig. 3. The geometry of the tin atom is a distorted tbp. The wider angle is N10–Sn16–C23 [147.4(1)°], whereas the equatorial angles are C17–Sn16–S15 109.2(2)°, S15–Sn16–C29 119.2(1)° and C17–Sn16–C29 111.5(2)°. The solid-state structure of compound **3** presents intramolecular hydrogen bonds, between C–H34 and N3, and CH7 and S14 [51].

Addition of DMSO-d_6 to **2** afforded compound **8**. The DMSO solutions gave two different polymorphs (**8a** and **8b**). The X-ray diffraction analyses showed the lead atoms hexacoordinated by the additional bonding of the DMSO oxygen atom. The S15–Pb–O angle is 174.1(1)° in **8a** and 171.3(1)° in **8b**, Fig. 4. The bond lengths of N10 → Pb

Table 5
Selected bond lengths and angles for **2**, **3**, **8**, **9**, **11**–**13**

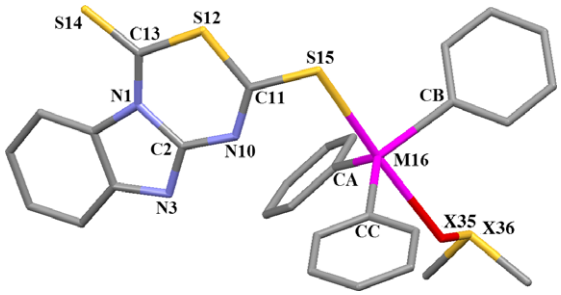

	2	**3**	**8a**	**8b**	**9**	**11**	**12**	**13** molecule 1	**13** molecule 2
N1–C2	1.42(1)	1.434(5)	1.437(7)	1.428(7)	1.44(1)	1.435(6)	1.444(4)	1.427(8)	1.433(9)
N1–C13	1.38(1)	1.361(6)	1.367(8)	1.366(7)	1.37(1)	1.358(6)	1.363(4)	1.38(1)	1.371(9)
N3–C2	1.28(1)	1.296(5)	1.289(7)	1.307(8)	1.30(1)	1.293(6)	1.296(4)	1.31(1)	1.312(8)
N10–C2	1.38(1)	1.368(5)	1.376(7)	1.364(8)	1.34(1)	1.356(7)	1.364(4)	1.356(9)	1.356(8)
N10–C11	1.29(1)	1.280(6)	1.284(7)	1.295(8)	1.28(1)	1.293(5)	1.291(5)	1.29(1)	1.293(8)
S12–C11	1.752(9)	1.754(5)	1.758(5)	1.751(5)	1.760(9)	1.756(5)	1.755(4)	1.757(7)	1.768(7)
S12–C13	1.733(9)	1.752(5)	1.742(6)	1.738(6)	1.74(1)	1.748(6)	1.740(3)	1.748(8)	1.736(7)
S14–C13	1.64(1)	1.632(5)	1.637(6)	1.640(6)	1.64(1)	1.640(5)	1.632(4)	1.630(7)	1.631(8)
S15–C11	1.727(7)	1.727(4)	1.721(5)	1.725(6)	1.71(1)	1.714(6)	1.714(3)	1.725(8)	1.711(7)
M16–S15	2.629(2)	2.478(1)	2.744(2)	2.684(2)	2.695(2)	2.596(1)	2.604(1)	2.615(2)	2.718(2)
M16–CA	2.179(8)	2.130(4)	2.176(5)	2.196(6)	2.17(1)	2.125(6)	2.131(3)	2.183(7)	2.192(8)
M16–CB	2.219(7)	2.143(4)	2.214(5)	2.211(6)	2.227(9)	2.146(5)	2.136(3)	2.209(7)	2.194(8)
M16–CC	2.175(8)	2.131(4)	2.185(5)	2.194(6)	2.171(9)	2.120(5)	2.130(3)	2.176(8)	2.196(7)
M16–N10	3.093(7)	3.088(3)	3.403(4)	3.400(5)	3.133(8)	3.112(4)	3.221(3)	3.170(5)	3.485(5)
M16–X35	3.607(3)		2.619(4)	2.628(4)	2.825(7)	2.656(3)	2.452(2)		2.624(6)
N10–C11–S15	122.5(7)	122.3(3)	123.8(4)	124.0(4)	123.8(7)	123.0(4)	122.9(3)	123.5(5)	125.7(6)
C11–S15–M16	95.6(3)	98.2(2)	101.0(2)	100.7(2)	95.1(3)	96.7(2)	99.8(1)	97.6(3)	103.5(2)
S15–M16–CA	103.8(2)	119.2(1)	103.1(1)	94.8(1)	98.2(2)	97.9(1)	99.35(8)	105.0(2)	103.8(2)
S15–M16–CB	95.8(2)	93.3(1)	92.0(1)	90.8(1)	91.7(2)	92.2(1)	85.7(1)	94.8(2)	87.2(2)
S15–M16–CC	103.3(2)	109.2(1)	94.9(1)	104.9(1)	99.3(2)	97.9(1)	94.7(1)	104.5(2)	96.67(19)
CA–M16–CB	112.4(3)	108.4(2)	109.2(2)	114.8(2)	111.9(3)	112.5(2)	117.9(1)	109.4(3)	112.5(3)
CA–M16–CC	127.0(3)	111.5(2)	123.9(2)	131.8(2)	128.7(4)	128.5(2)	125.7(1)	124.9(3)	125.4(3)
CB–M16–CC	109.0(3)	114.1(2)	123.0(2)	108.5(2)	115.3(4)	115.5(2)	115.3(1)	113.4(3)	118.7(3)
S15–M16–X35	173.60(7)		174.1(1)	171.3(1)	175.9(2)	177.1(1)	174.44(5)		171.3(1)
CA–M16–X35	81.6(2)		82.8(2)	80.4(2)	78.1(3)	79.6(2)	84.12(9)		81.4(2)
CB–M16–X35	85.2(2)		85.5(2)	84.8(2)	91.2(3)	90.2(1)	88.9(1)		84.4(2)
CC–M16–X35	70.5(2)		82.1(2)	83.7(2)	82.1(3)	82.7(1)	86.7(1)		85.6(2)
M16–X35–X36			121.1(2)	149.8(2)			145.9(1)		

are 3.403(4) Å **8a** and 3.400(5) Å **8b**, and those of S15–Pb are 2.744(2) Å (**8a**) and 2.684(2) Å (**8b**). Both, the N10–Pb and S–Pb bond lengths are longer in **8** than in **2** [3.093(7) and 2.629(2) Å] which could be the effect of a strong O–Pb coordination bond [Pb–O 2.619(4) Å **8a**, Pb–O 2.628(4) Å **8b**], Fig. 4.

In the cell of polymorph **8a**, dimers are formed by bifurcated C–H···O···H–C hydrogen bonds [2.81(6) and 2.59(7) Å] of the coordinated DMSO group, the angle Pb–O–S is 121.1(2)°. The sulfur atom of the coordinated DMSO is pyramidal [O35–S36–C37 angle is 106.3(3)° and O35–S36–C38 is 104.7(3)°], Fig. 5.

The second polymorph (**8b**) forms dimers by two bifurcated C–H···N···H–C bonds (2.49 and 2.53 Å), Fig. 6. The oxygen has some sp character as is deduced from the open angle Pb–O35–S36 149.8(2)°. A polymer is formed by π-stacking between the tricycles, Fig. 7.

Addition of pyridine to the lead compound **2** afforded adduct **9**. In the crystal the lead atom is hexacoordinated, Fig. 8. The sulfur and the pyridine nitrogen are *trans* [S–Pb–N angle is 175.9(2)° and bond lengths are N35–Pb 2.825(7) and S–Pb 2.695(2) Å]. The planes of the pyridine and the ligand are orthogonal. One Pb–Ph group is aligned with the S–Pb–N bonds, giving two hydrogen bonds [CH28···S15 2.71 Å and CH24···N35(π) 2.63 Å] [51], Fig. 8. One molecule of pyridine (not shown) cocrystallized with **9**.

The solid-state structure of the tin compound **11** is isomorphous with that found for the analogous lead compound **9**, Fig. 9. The Sn–N 2.656(3) Å and Sn–S 2.596(1) Å bond distances are shorter than in compound **9**. One of the Sn–Ph groups is aligned with S15–Sn–N35 bonds and its *ortho*-protons form hydrogen bonds with S15 (2.61 Å) and N35 (2.56 Å). The other two phenyl

Table 6
Crystal and data collection parameters of compounds **2**, **3** and **8**

Compound	**2**	**3**	**8a**	**8b**
Formula	$C_{27}H_{19}N_3PbS_3$	$C_{27}H_{19}N_3S_3Sn_1$	$C_{29}H_{25}N_3OPbS_4$	$C_{29}H_{25}N_3OPbS_4$
Formula weight	688.87	600.36	767	767
Temperature (K)	293	293	293	293
Wavelength (Å)	0.71073	0.71073	0.71073	0.71073
Crystal system	Triclinic	Triclinic	Monoclinic	Monoclinic
Space group	$P\bar{1}$	$P\bar{1}$	$P2_1/c$	$C2/c$
a (Å)	13.1004(2)	9.7456(2)	15.3021(2)	25.5478(3)
b (Å)	13.8576(2)	10.0928(3)	10.63410(10)	11.9678(2)
c (Å)	15.6071(2)	13.5582(4)	18.0650(2)	19.1624(2)
α (°)	71.6889(6)	92.382(2)	90	90
β (°)	71.3255(6)	93.042(2)	97.3826(6)	101.2913(7)
γ (°)	84.7972(6)	109.8716(15)	90	90
Volume (Å^3)	2548.08(6)	1249.89(6)	2915.24(6)	5745.52(13)
Z	4	2	4	8
D_{calc} (Mg/m^3)	1.796	1.595	1.747	1.773
μ (mm^{-1})	6.89	1.29	6.10	6.19
Absorption correction	Multiscan	SADABS	Multiscan	SADABS
$T_{maximum}$, $T_{minimum}$	0.5, 0.21	0.94, 0.68	0.16, 0.09	0.54, 0.4
$F(000)$	1328	600	1496	2992
Crystal size (mm)	0.3 × 0.22 × 0.1	0.25 × 0.2 × 0.05	0.5 × 0.38 × 0.3	0.3 × 0.15 × 0.1
Crystal color	Yellow	Yellow	Yellow	Yellow
θ Range	1.55–28.71	1.51–28.67	2.27–28.71	1.62–28.69
Index range	$-17 \leqslant h \leqslant 17$, $-18 \leqslant k \leqslant 18$, $-16 \leqslant l \leqslant 21$,	$-12 \leqslant h \leqslant 12$, $-13 \leqslant k \leqslant 11$, $-18 \leqslant l \leqslant 18$,	$-19 \leqslant h \leqslant 20$, $-13 \leqslant k \leqslant 14$, $-24 \leqslant l \leqslant 24$,	$-33 \leqslant h \leqslant 33$ $-16 \leqslant k \leqslant 14$ $-25 \leqslant l \leqslant 25$
Reflections collected	51 706	13 123	58 463	52 064
Independent reflections	13 105	6278	7532	7401
R_{int}	0.095	0.062	0.116	0.088
Completeness to θ (°)	28.13, 99.8%	26.66, 98.3%	28.71, 99.7%	28.69, 99.8%
Observed reflections	6289	3962	4183	4075
Goodness-of-fit on F^2	1.04	1.07	1.06	1.02
Final R_1	0.036 ($I > 3.0\sigma$)	0.038 ($I > 3.0\sigma$)	0.027 ($I > 3.0\sigma$)	0.024 ($I > 3.0\sigma$)
Final wR_2	0.042	0.044	0.028	0.028

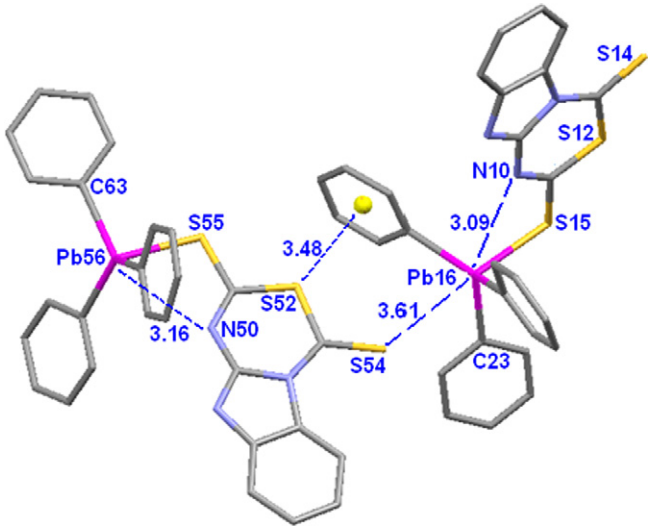

Fig. 1. Asymmetric unit of compound **2**. A polymer is formed by intermolecular S → Pb coordination and S → π interactions.

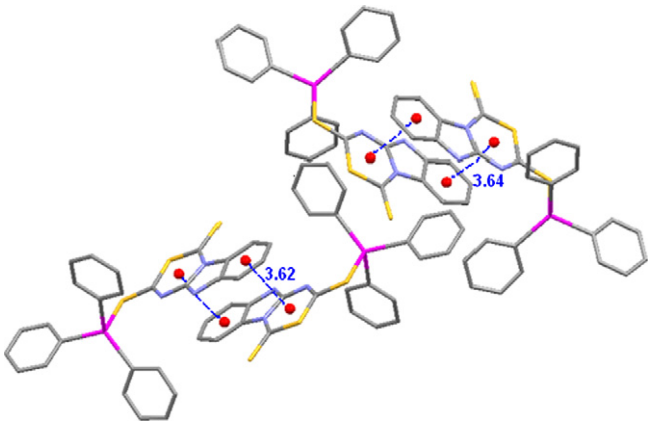

Fig. 2. Intermolecular π-stacking in **2**.

groups lie almost in the equatorial plane. An *ortho* proton (H30) of one of these groups forms bifurcated hydrogen bonds with N3 (2.91 Å) and N10 (2.76 Å). A molecule of pyridine (not shown in Fig. 9) co-crystallized with **11** (see Table 7).

Tin compound **14** is coordinated to the oxygen atom of the triphenylphosphine oxide. The oxygen O35 and the sulfur S15 are *trans* [O–Sn 2.452(2) Å and S–Sn 2.604(1) Å]. The Sn–N10 coordination bond length is 3.221(3) Å. Angle S15–Sn–O35 is 174.44(5)° and Sn–O35–P36 is 145.9(1)°. The phosphorus atom is tetrahedral, Fig. 10.

Compound **16** was obtained from a solution of **2** in wet methanol. There are two different lead molecules in the cell,

one is compound **2**, whose structural data are similar to that found in the crystal of **2**, Table 5. The other is compound **16**, which has a water molecule coordinated to the lead, in *trans* position to the sulfur atom, Fig. 11. In compound **16**, the distance between N50 and Pb56 is 3.485(5) Å and the bond lengths are S55–Pb56 [2.718(2) Å] and O75–Pb56 [2.624(6) Å]. The effect of the water strong coordination is observed in the lengths of N–Pb and S–Pb bonds which are longer in **16** than in the compound **2** co-crystallized with **16** [S15–Pb16 2.615(2) and N10–Pb16 3.170(5) Å].

In the structure of **16**, one of the Pb-phenyl groups is aligned with the axis S–Pb–O, in such a way that the *o*-phenyl protons form hydrogen bonds with S55 (2.86 Å) and O75 (2.40 Å), Fig. 12. Bifurcated π-interactions are represented in Fig. 13, they are formed between C45 of a molecule of **16** and C2 of a molecule of **2** [3.38(1) Å] [50] and the C45H proton with the π electrons of C17 (2.886 Å) [51].

Another intermolecular association between two molecules of compound **16** is produced by hydrogen bonds between one proton of a coordinated water molecule with the oxygen of a crystallization water molecule, whose proton is in turn coordinated to N43 of another molecule of **16**, Fig. 14.

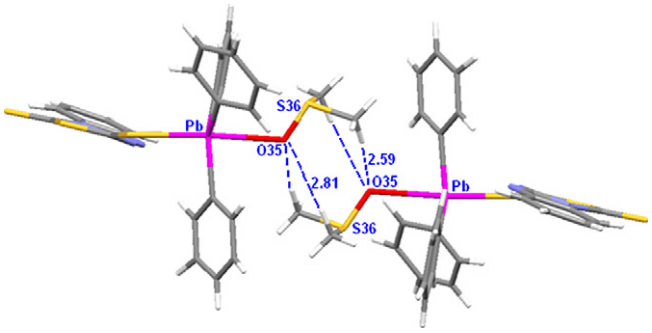

Fig. 5. Dimer formed in polymorph **8a** by C–H···O hydrogen bonds.

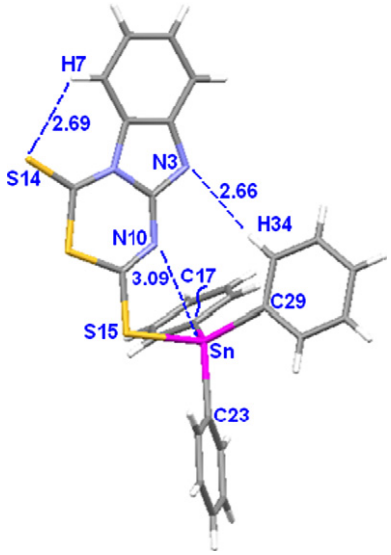

Fig. 3. Solid-state structure of compound **3**. The tin has a distorted tbp geometry with N10 and C23 as the apical atoms. The N → Sn coordination and two intramolecular hydrogen bonds are shown.

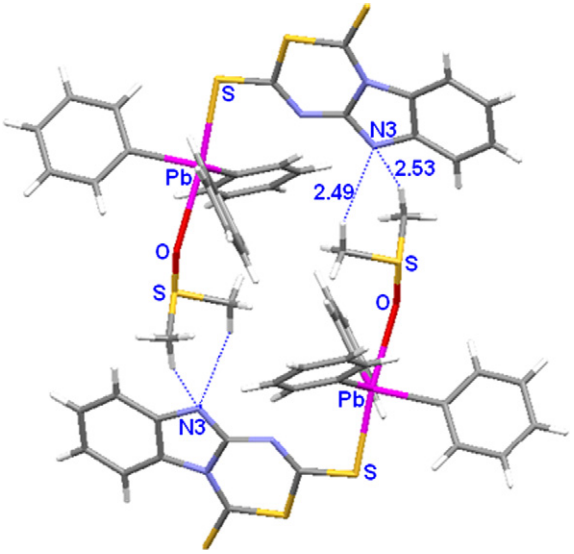

Fig. 6. Dimer formed in polymorph **8b**.

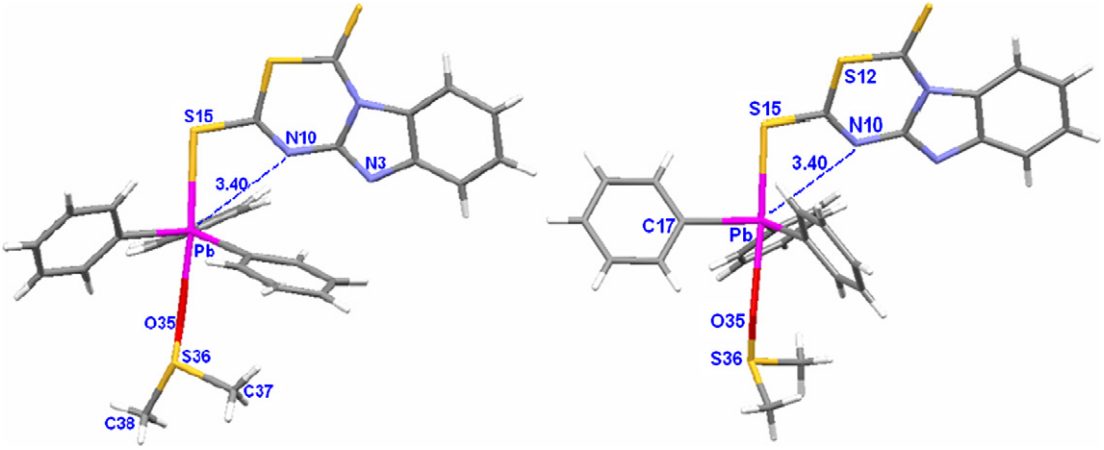

Fig. 4. Solid-state structure of polymorphs **8a** (left) and **8b** (right).

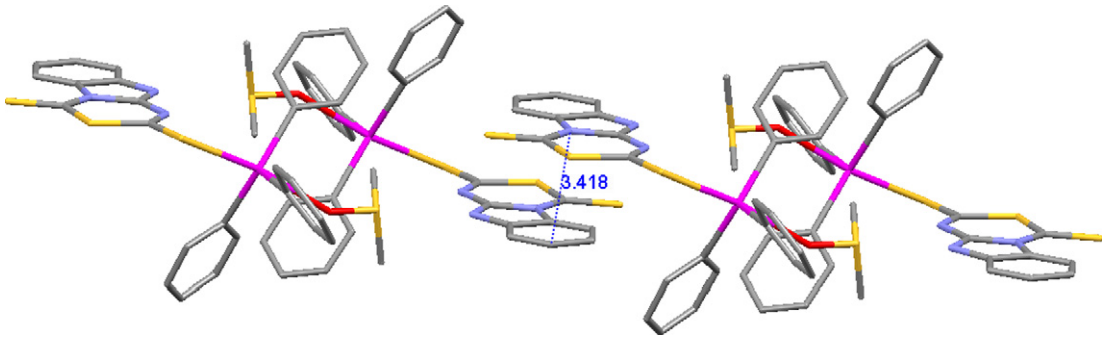

Fig. 7. In **8b** dimers form a polymer by π-stacking [distance N1···C5 3.418(8) Å].

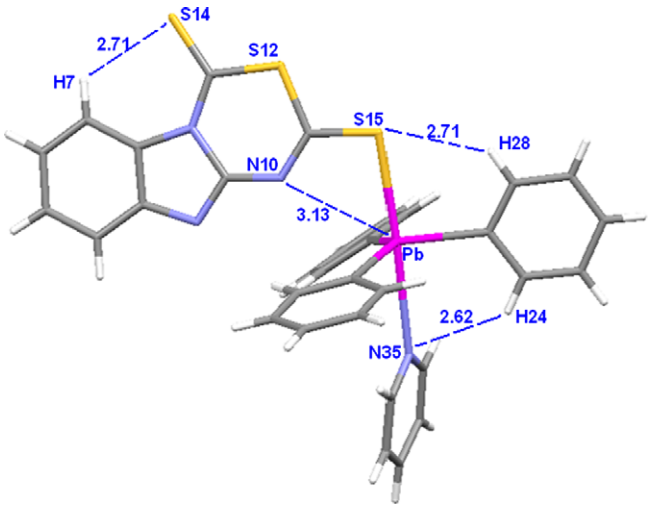

Fig. 8. Solid-state structure of compound **9**.

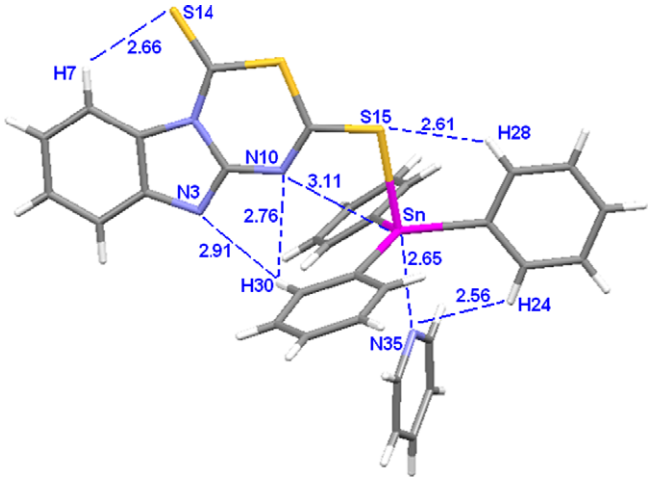

Fig. 9. Solid-state structure of compound **11.**

An interesting fact is observed in the co-crystal of **2** with **16**. Two molecules of **2** form a dimer by intermolecular π-interactions (3.71 Å) between carbon atoms C29–C30 of two Pb–Ph groups marked as **A** in Fig. 15. The short distances (3.81–3.89 Å, $\sum_{vwr} = 4.1$ Å) between the Pb atoms and the π electrons of the C31–C32 bond, marked as **B** and C–H31···C18 π-interaction (2.8 Å) marked as **C** further stabilize the dimeric structure.

3. Summary

Metathesis reactions of the new tricyclic and polyfunctional compound potassium 4-thioxo-3-thia-1,4a,9-triazafluorene-2-thiolate with Ph_3PbCl, Ph_3SnCl and Ph_3GeCl provided metal pentacoordinated compounds, by bidentate coordination of the ligand. The products, in the presence of Lewis bases, gave a series of hexacoordinated compounds. Lead compounds are very stable to open air manipulations, whereas tin compounds are susceptible to hydrolysis. The germanium compound **4** was very reactive to moisture and was decomposed by addition of Lewis bases even in dry conditions. ^{119}Sn and ^{207}Pb NMR data were fundamental for evaluation of metal atom coordination in solution, which was also confirmed in the solid-state by X-ray diffraction. In all compounds, the ligand prefers bonding with the metal atoms through S15 which allows a weak coordination of N10 forming a four membered metallacycle.

4. Experimental

4.1. General comments

Vacuum line techniques were employed for all manipulations of air and moisture sensitive compounds. THF was dried by distillation from sodium–benzophenone under nitrogen atmosphere prior to use. Dry DMSO-d_6, pyridine-d_5, CD_3OD, THF-d_8 and organolead, organotin and organogermanium were purchased from Aldrich and used without further purification. The melting points were obtained on a Mel-Temp II apparatus and are uncorrected. Mass spectra in the EI mode were recorded at 20 eV on a Hewlett–Packard HP 5989 spectrometer. High resolution mass spectra were obtained by LC/MSD TOF on Agilent Technologies instrument with APCI as ionization source. Elemental analyses were performed on Eager 300 equipment. NMR spectra were obtained on a Jeol GSX-270, Jeol Eclipse 400 MHz and Bruker Advance 300 MHz.

Table 7
Crystal and data collection parameters of compounds **9**, **11**, **14** and **16**

	9	**11**	**14**	**16**
Formula	$2(C_{32}H_{24}N_4PbS_3)\cdot C_5H_5N$	$2(C_{32}H_{24}N_4SnS_3)\cdot C_5H_5N$	$C_{45}H_{34}N_3OPS_3Sn$	$C_{27}H_{21}N_3OPbS_3\cdot C_{27}H_{19}N_3PbS_3\cdot CH_4O\cdot H_2O$
Formula weight	1615.04	1438.02	878.65	1445.8
Temperature (K)	293	293	293	293
Wavelength (Å)	0.71073	0.71073	0.71073	0.71073
Crystal system	Monoclinic	Monoclinic	Monoclinic	Triclinic
Space group	$P2_1/c$	$P2_1/c$	$P2_1/n$	$P\bar{1}$
a (Å)	9.94200(10)	9.93460(10)	12.03330(10)	13.2869(2)
b (Å)	23.8990(3)	23.8530(4)	10.77470(10)	14.2793(3)
c (Å)	16.8289(2)	16.8665(2)	30.8810(3))	16.0323(5)
α (°)	90	90	90	91.6002(8)
β (°)	124.2940(10)	125.0000(10)	93.6861(4)	90.9159(8)
γ (°)	90	90	90	114.5976(13)
V (Å^3)	3303.48(8)	3273.84(8)	3995.60(6)	2763.39(12)
Z	2	2	4	2
$D_{calc.}$ (Mg/m^3)	1.624	1.459	1.461	1.737
μ (mm^{-1})	5.327	1.00	0.88	6.359
Absorption correction	Multiscan	SADABS	SADABS	SADABS
$T_{maximum}$, $T_{minimum}$	0.45, 0.26	0.82, 0.59	0.79, 0.89	0.73, 0.5
$F(000)$	1580	1452	1784	1404
Crystal size (mm)	0.28 × 0.25 × 0.15	0.25 × 0.25 × 0.2	0.5 × 0.38 × 0.3	0.25 × 0.1 × 0.05
Crystal color	Yellow	Yellow	Yellow	Yellow
θ range	1.69–28.71	1.70–30.51	1.32–30.14	3.09–30.49
Index range	$-13 \leqslant h \leqslant 13$, $-32 \leqslant k \leqslant 32$, $-21 \leqslant l \leqslant 22$,	$-11 \leqslant h \leqslant 13$, $-33 \leqslant k \leqslant 33$, $-24 \leqslant l \leqslant 23$,	$-19 \leqslant h \leqslant 20$, $-13 \leqslant k \leqslant 14$, $-24 \leqslant l \leqslant 24$,	$-18 \leqslant h \leqslant 18$ $-15 \leqslant k \leqslant 20$ $-21 \leqslant l \leqslant 22$
Reflections collected	37493	36297	79084	49813
Independent reflections	8511	9162	10836	15337
R_{int}	0.116	0.082	0.101	0.061
Completeness to θ (°)	28.71, 99.6%	25.02, 99.5%	28.33, 99.6%	25.00, 99.4%
Observed reflections	3202	3528	4575	6311
Goodness-of-fit on F^2	1.08	1.09	1.05	1.03
Final R_1	0.036 ($I > 2.5\sigma$)	0.033 ($I > 2.5\sigma$)	0.027 ($I > 2.5\sigma$)	0.033 ($I > 2.5\sigma$)
Final wR_2	0.038	0.038	0.029	0.034

Coordination compounds **5**–**16** were submitted to high resolution mass analyses, however all compounds dissociate in the equipment and the molecular masses were not obtained

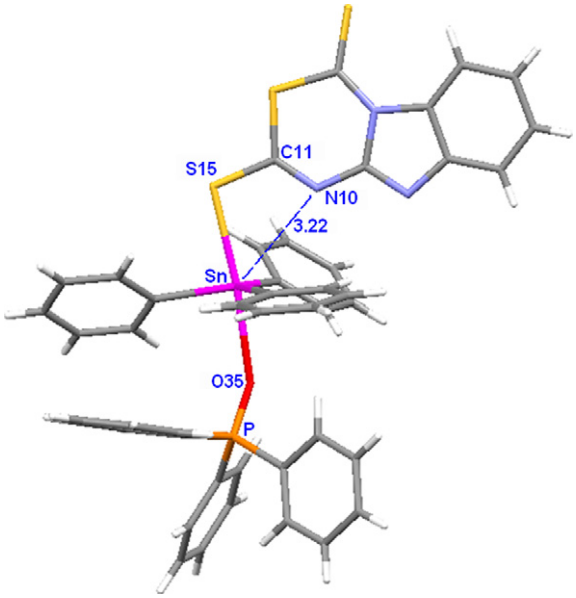

Fig. 10. Solid-state structure of compound **14**.

4.2. Syntheses

4.2.1. Potassium 4-thioxo-3-thia-1,4a,9-triaza-fluorene-2-thiolate (*1b*)

To a solution of 20 g (150 mmol) of 2-aminobenzimidazole in 200 mL of DMF, powdered KOH was added (28.1 g, 150 mmol, 90%). The reaction mixture was stirred for 4 h. Then 20 mL of CS_2 were added (167 mmol) and stirring continued. After 12 h, $CHCl_3$ (1 L) was added and then the precipitate filtered. The solid was washed with water (500 mL), left to dry and dissolved in acetone and set aside. After 15 days, a microcrystalline yellow powder was obtained (17.2 g, 35%), which was the dihydrate of **1**. Dec. at 300 °C. Anal. Calc. for $C_9H_4N_3S_3\ K\cdot 2H_2O$: C, 33.21; H, 2.48; N, 12.91; S 29.55. Found: C, 33.58; H, 2.48; N, 13.07; S, 29.92%.

4.2.2. 9H-3-Thia-1,4a,9-triaza-fluorene-2,4-dithione (*1a*)

Compound **1b** (3 g, 9.2 mmol) was dissolved in THF (50 mL) and HCl (aq, 36%, 3 mL, 35 mmol) was added. The precipitate was filtered and left to dry to give a yellow powder. (2.2 g, 95%). M.p.: 158–162 °C. MS (EI, 20 eV): [M$^+$] 251(3) *m/z*. Anal. Calc. for $C_9H_5N_3S_3$: C, 43.01; H, 2.01; N, 16.72; S 38.27. Found: C, 43.18; H, 1.94; N, 16.61; S, 37.66%.

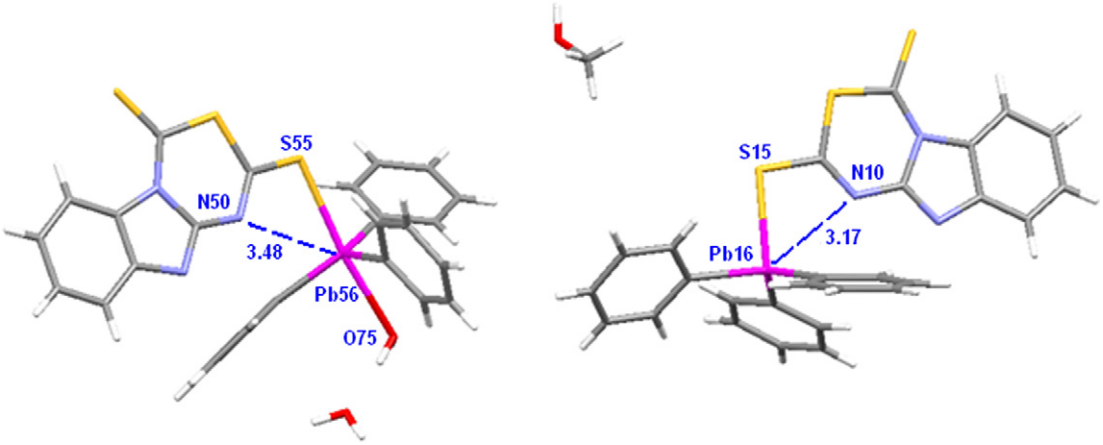

Fig. 11. View of the asymmetric unit of **16** co-crystallized with one molecule of **2**, one of methanol and one of water.

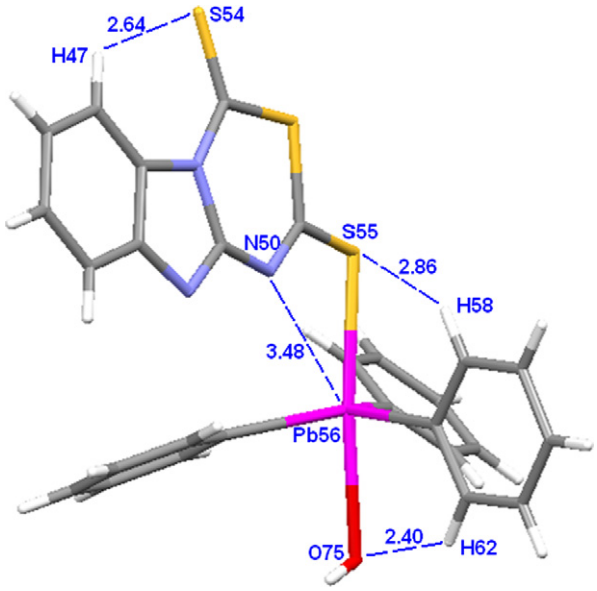

Fig. 12. Structure of compound **16** showing the intramolecular hydrogen bonds and the N–Pb coordination bond.

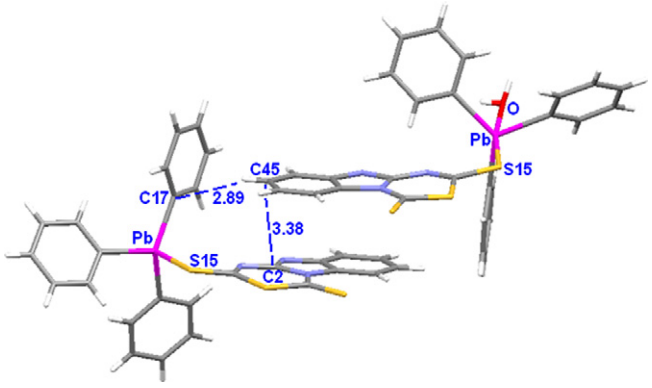

Fig. 13. Intermolecular π-interactions in the co-crystal of compounds **16** and **2**.

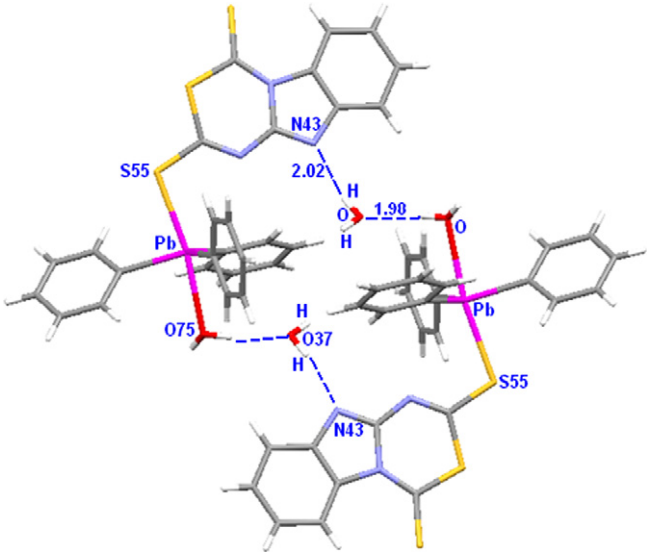

Fig. 14. Intermolecular association of two molecules of **16** by two hydrogen bonds of two water molecules.

*4.2.3. Triphenyllead 4-thioxo-3-thia-1,4a,9-triaza-fluorene-2-thiolate (**2**)*

Compound **1** (500 mg, 1.54 mmol) was dried at 200 °C in a vacuum line for 2 h. Then it was dissolved in dried THF (50 mL) and Ph_3PbCl was added (730 mg, 1.54 mmol) and stirred overnight. The mixture was set aside for 6 h in order to separate the liquid from the solid, then the liquid was evaporated to give a yellow solid (895 mg, 84%). M.p.: 183–186 °C. Suitable crystals for X-ray were grown from $CHCl_3$ or THF solutions. HRMS (TOF), $(C_{27}H_{19}N_3S_3Pb\text{-}H)^+$ 690.0580 amu. Found: 690.0579 (error = 0.19 ppm). Anal. Calc. for $C_{27}H_{19}N_3S_3Pb$: C, 47.08; H, 2.78; N, 6.10; S 13.96. Found: C, 46.86; H, 2.80; N, 5.95; S, 13.26%.

*4.2.4. Triphenyltin 4-thioxo-3-thia-1,4a,9-triaza-fluorene-2-thiolate (**3**)*

The same procedure as for compound **2** was used for **3**. Compound **1** (500 mg, 1.54 mmol) and Ph_3SnCl (594 mg,

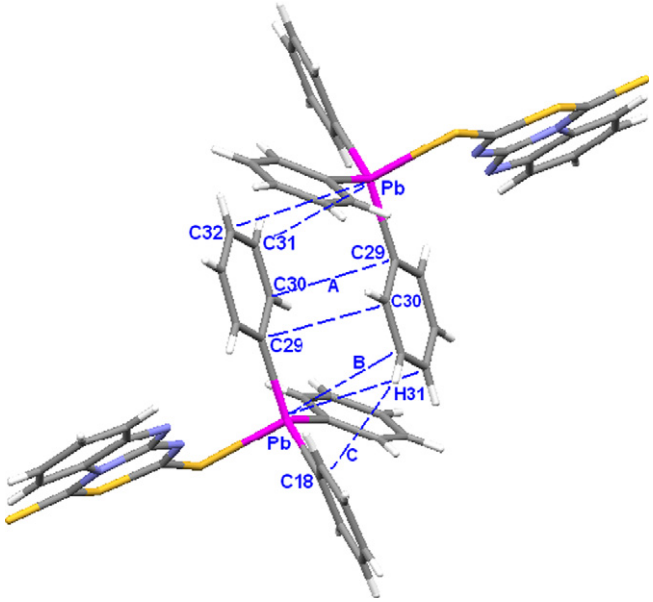

Fig. 15. Dimer of compound **2** formed in the co-crystal of **2** and **16**, by cooperative π-interactions between C29···C30 (3.71 Å), marked as A, between Pb and C32–C31 (3.81 and 3.89 Å) B, and between H31 and C18 (2.83 Å), C.

1.54 mmol) afforded a microcrystalline yellow powder (740 mg, 80%). M.p.: 166–168 °C. Crystals for X-ray diffraction were grown from a solution in THF. HRMS (TOF) $(C_{27}H_{19}N_3S_3Sn\text{-}H)^+$ 601.9835 amu. Found: 601.9854 (error = 3.01 ppm).

*4.2.5. Triphenylgermanium 4-thioxo-3-thia-1,4a, 9-triaza-fluorene-2-thiolate (**4**)*

The same procedure as for compound **2** was used for **4**. Compound **1** (500 mg, 1.54 mmol) and Ph_3GeCl (521 mg, 1.54 mmol) afforded a yellow powder (570 mg, 67%). Dec. at 160 °C. HRMS (TOF) $(C_{27}H_{19}N_3S_3Ge\text{–}H)^+$ 556.0025. Found: 556.0030 (error = 0.78 ppm).

*4.2.6. (O–Pb)-tetrahydrofurane-4-thioxo-3-thia-1,4a, 9-triaza-fluorene-2-thiolate-triphenyllead (**5**), (O–Sn)-tetrahydrofurane-4-thioxo-3-thia-1,4a, 9-triaza-fluorene-2-thiolate triphenyltin (**6**) (O–Ge)-tetrahydrofurane-4-thioxo-3-thia-1,4a, 9-triaza-fluorene-2-thiolate triphenylgermanium (**7**)*

Solutions of 20 mg of **2** (29.0 μmol), **3** (33.2 μmol) or **4** (36.1 μmol) in 0.4 mL of dry THF-d_8 were analyzed by NMR. Evaporation of the solvent afforded compounds **2** and **3**, whereas compound **4** decomposes on standing or by solvent evaporation.

*4.2.7. (O–Pb)-dimethylsulfoxide-4-thioxo-3-thia-1,4a, 9-triaza-fluorene-2-thiolate-triphenyllead (**8**)*

A solution of **2** (50 mg, 72.6 μmol) dissolved in 0.4 mL of DMSO-d_6 afforded compound **8**, which was analyzed by NMR. After two weeks pale yellow crystals (**8b**) were formed in the NMR tube. M.p.: 139–141 °C. From a mixture of compound **2**, with 2 equiv. of ligand **1** in DMSO set aside for three months, pale yellow crystals of the polymorph **8a** were obtained, M.p.: 154 °C. Both polymorphs were submitted to X-ray diffraction analyses.

*4.2.8. (N–Pb)-pyridine-4-thioxo-3-thia-1,4a, 9-triaza-fluorene-2-thiolate-triphenyllead (**9**)*

A solution of 50 mg of **2** (72.6 μmol) dissolved in 0.4 mL of pyridine-d_5 produced compound **9** which was studied by NMR. After one day yellow crystals were formed that were used for X-ray diffraction analyses. Decomp. at 130 °C.

*4.2.9. (O–Sn)-dimethylsulfoxide-4-thioxo-3-thia-1,4a,9-triaza-fluorene-2-thiolate-triphenyltin (**10**)*

A solution of **3** (50 mg, 83.3 μmol) dissolved in 0.4 mL of DMSO-d_6 gave compound **10**, the yellow solution was submitted to NMR analyses, no crystals were obtained.

*4.2.10. (N–Sn)-pyridine-4-thioxo-3-thia-1,4a, 9-triaza-fluorene-2-thiolate-triphenyltin (**11**)*

A solution of **3** (50 mg, 83.3 μmol) dissolved in 0.4 mL of pyridine-d_5, produced compound **11**, which was submitted to NMR analyses. After three days yellow crystals were formed in the tube, which were suitable for X-ray diffraction analyses. M.p.: 175–176 °C.

*4.2.11. (O–Pb)-triphenyphosphine-oxide-4-thioxo-3-thia-1,4a,9-triaza-fluorene-2-thiolate-triphenyllead (**12**) and (O–Sn)-triphenyphosphine-oxide-4-thioxo-3-thia-1,4a,9-triaza-fluorene-2-thiolate-triphenyltin (**14**)*

To a solution of compound **2** (20 mg, 29 μmol) in $CDCl_3$ or **3** (20 mg, 33.2 μmol) in THF, approx. 10 equiv. of Ph_3PO were added (81 mg, 290 μmol). The yellow solutions were submitted to NMR. An equimolar mixture of **3** (20 mg, 33.2 μmol) and Ph_3PO (9.2 mg, 33.2 μmol) in 0.4 mL of THF-d_8 afforded pale yellow crystals suitable for X-ray diffraction analyses. M.p.: 154–158 °C.

*4.2.12. (O–Pb)-methanol-4-thioxo-3-thia-1,4a,9-triaza-fluorene-2-thiolate-triphenyllead (**13**) and (O–Pb)-water-4-thioxo-3-thia-1,4a,9-triaza-fluorene-2-thiolate-triphenyllead (**16**)*

Complex **13** was prepared by dissolution of compound **2** (5 mg, 7.3 μmol) in CD_3OD, and characterized by NMR analyses. From the NMR tube pale yellow crystals were obtained for X-ray diffraction analyses which corresponded to a co-crystal of compounds **16** and **2**. M.p.: 138–146 °C.

*4.2.13. (O–Sn)-methanol-4-thioxo-3-thia-1,4a,9-triaza-fluorene-2-thiolate- triphenyltin (**15**)*

Complex **15** was prepared from a solution of compound **3** (5 mg, 8.3 μmol) in 0.4 mL of CD_3OD and characterized by NMR analyses.

4.3. X-ray structural analysis of compounds **2**, **3**, **8**, **9**, **11**, **14** and **16**

Data were measured on a Nonius Kappa CCD instrument with CCD area detector using graphite-monochromated Mo Kα radiation at 293 K. Intensities were measured using $\varphi + \omega$ scans. All structures were solved using direct methods with SHELX-97 [52], except compound **2** which was solved using SIR-2002 [53]. The refinement for all structures (based on F^2 of all data) was performed by full matrix least-squares techniques with crystals 12.84 [54].

All non-hydrogen atoms were refined anisotropically, all C–H hydrogen atoms were placed on ideal positions, and the O–H of **16** were located in the difference map and allowed to ride on their respective atoms.

Acknowledgements

Financial support from Conacyt-Mexico and Cinvestav is acknowledged as well as Conacyt-Mexico scholarships for A.E.-R. and A.P-H. The authors are grateful to A. Paz-Sandoval and J. Guthrie for valuable comments discussions.

Appendix A. Supplementary material

CCDC 666737, 666738, 666739, 666740, 666741, 666742, 666743 and 666744 for compounds **2**, **3**, **8a**, **8b**, **9**, **11**, **12** and **16**. These data can be obtained free of charge from The Cambridge Crystallographic Data Centre via www.ccdc.cam.ac.uk/data_request/cif. Supplementary data associated with this article can be found, in the online version, at doi:10.1016/j.jorganchem.2007.11.040.

References

[1] C. Camacho-Camacho, R. Contreras, H. Nöth, M. Bechmann, A. Sebald, W. Milius, B. Wrackmeyer, Magn. Reson. Chem. 40 (2002) 31.
[2] C. Camacho-Camacho, V.M. Jiménez-Pérez, J.C. Gálvez-Ruiz, A. Flores-Parra, R. Contreras, J. Organomet. Chem. 691 (2006) 1590.
[3] C. Camacho-Camacho, H. Tlahuext, H. Nöth, R. Contreras, Heteroatom. Chem. 9 (1997) 321.
[4] M.P. Fialon, N. Andrade-López, N. Barba-Behrens, R. Contreras, Heteroatom Chem. 9 (1998) 637.
[5] R. Contreras, V.M. Jiménez-Pérez, C. Camacho-Camacho, M. Güizado-Rodríguez, B. Wrackmeyer, J. Organomet. Chem. 604 (2000) 229.
[6] V.M. Jiménez-Pérez, C. Camacho-Camacho, M. Güizado-Rodríguez, H. Nöth, R. Contreras, J. Organometal. Chem. 614/615 (2000) 283.
[7] V.M. Jiménez-Pérez, A. Ariza-Castolo, A. Flores-Parra, R. Contreras, J. Organometal. Chem. 691 (2006) 1584.
[8] V.M. Jiménez-Pérez, C. Camacho-Camacho, A. Ramos-Organillo, R. Ramírez-Trejo, A. Peña-Hueso, R. Contreras, A. Flores-Parra, J. Organometal. Chem. 692 (2007) 5549.
[9] Saul Patai, The Chemistry of Functional Groups: The Chemistry of Organic Germanium, Tin and Lead Compounds, vol. 19, Wiley, 1995 (Chapter 19).
[10] J. Parr, in: J.A. MacCleverty, T.J. Meyer (Eds.), Comprehensive Coordination Chem. II, vol. 3, Elsevier Pergamon, 2004, p. 545.
[11] T. Sato, in: E.W. Abel, F.G.A. Stone, G. Wilkinson (Eds.), Comprehensive Organometal. Chem. II, vol. 11, Pergamon Press, 1995, p. 389 (Chapter 8).
[12] J.T. Pinhey, in: E.W. Abel, F.G.A. Stone, G. Wilkinson (Eds.), Comprehensive Organometal. Chem. II, vol. 11, Pergamon Press, 1995, p. 461 (Chapter 11).
[13] A.G. Davies, Organotin Chemistry, VCH, 1997.
[14] R.V. Singh, S.C. Joshi, A. Gajraj, P. Nagpal, Appl. Organometal. Chem. 16 (2002) 713.
[15] S. Tabassum, C. Pettinari, J. Organomet. Chem. 691 (2006) 1761.
[16] C. Pellerito, L. Nagy, L. Pellerito, A. Szorcsik, J. Organomet. Chem. 691 (2006) 1733.
[17] F. Huber, G. Roge, L. Carl, G. Atassi, F. Spreáfico, S. Filippeschi, R. Barbieri, A. Silvestri, E. Rivarola, G. Ruisi, F. Di Bianca, G. Alonzo, J. Chem. Soc., Dalton Trans (1985) 523.
[18] J.S. Magyar, T.-C. Weng, C.M. Stern, D.F. Dye, B.W. Rous, J.C. Payne, B.M. Bridgewater, A. Mijovilovich, G. Parkin, J.M. Zaleski, J.E. Penner-Hahn, H.A. Godwin, J. Am. Chem. Soc. 127 (2005) 9495.
[19] Agency for Toxic Substances and Disease Registry. (<http://www.atsdr.cdc.gov>).
[20] A.B. Ghering, L.M.M. Jenkins, B.L. Schenck, S. Deo, R.A. Mayer, M.J. Pikaart, J.G. Omichinski, H.A. Godwin, J. Am. Chem. Soc. 127 (2005) 3751.
[21] R.J. Andersen, R.C. diTargiani, R.D. Hancock, C.L. Stern, D.P. Goldberg, H.A. Godwin, Inorg. Chem. 45 (2006) 6574.
[22] R.R. Moskalyk, Miner. Eng. 17 (2004) 393.
[23] K. Rubina, E. Abele, P. Arsenyau, R. Abele, M. Veveris, E. Lukevics, Met. Based Drugs 8 (2001) 85.
[24] G.B. Gerber, A. Leonard, Mutat. Res. 387 (1997) 141.
[25] G. Rima, J. Satgé, R. Dagiral, C. Lión, H. Sentenac-Roumanou, M. Fatome, V. Roman, J.-D. Laval, Eur. J. Med. Chem. 6 (1999) 49.
[26] W.L. Drew, R.C. Miner, G.I. Marousek, S. Chou, J. Clin. Virol. 37 (2006) 124.
[27] I. Omar, T.M. O'Neill, S. Rossall, Plant Pathol. 55 (2006) 92.
[28] A. Joubert, X.-W. Sun, E. Johansson, C. Bailly, J. Mann, S. Neidle, Biochemistry 42 (2003) 5984.
[29] A.V. Dolzhenko, W.-K. Chui, J. Heterocyclic Chem. 43 (2006) 95.
[30] A.V. Dolzhenko, W.-K. Chui, A.V. Dolzhenko, Heterocyclic Chem. 43 (2006) 1513.
[31] A.D. Settimo, G. Primofiore, F.D. Settimo, A.M. Marini, S. Taliani, S. Salerno, L.D. Via, J. Heterocyclic Chem. 40 (2003) 1091.
[32] F. Saczewski, J. Saczewski, M. Gdaniec, J. Org. Chem. 68 (2003) 4791.
[33] M. Witanowski, L. Stefaniak, Annu. Rep. NMR Spectrosc. 18 (1986) 67.
[34] A.E. Cisneros-Gómez, A. Ramos-Organillo, J. Hernández-Díaz, J. Nieto-Martínez, R. Contreras, S.E. Castillo-Blum, Heteroatom Chem. 11 (2000) 392.
[35] E.S. Raper, Coord. Chem. Rev. 153 (1996) 199.
[36] B. Wrackmeyer, K. Horchler, Annu. Rep. NMR Spectrosc. 22 (1989) 249.
[37] P.J. Smith, A.P. Tupciauskas, Annu. Rep. NMR Spectrosc. 8 (1978) 291.
[38] B. Wrackmeyer, Annu. Rep. NMR Spectrosc. 38 (1999) 203.
[39] B. Wrackmeyer, Annu. Rep. NMR Spectrosc. 16 (1985) 73.
[40] R. Hani, R.A. Geanangel, Coord. Chem. Rev. 44 (1982) 229.
[41] J. Holecek, M. Nadvornik, K. Handlir, A. Lycka, J. Organometal. Chem. 241 (1983) 177.
[42] M.G. Begley, G. Gaffney, P.G. Harrison, A. Steel, J. Organometal. Chem. 289 (1985) 281.
[43] A. Kalsoom, M. Mazhar, S. Ali, M.F. Mahon, K.C. Molloy, M.I. Chaudry, Appl. Organometal. Chem. 11 (1997) 47.
[44] Y. Shi, C. Ma, R. Zhang, J. Organometal. Chem. 691 (2006) 1661, and references cited there.
[45] J.S. Casas, A. Castineiras, E.G. Martínez, A.S. González, A. Sordo, Polyhedron 16 (1997) 795.
[46] C. Ma, Y. Shi, Q. Jiang, Heteroatom Chem. 16 (2005) 69.

[47] M. Barret, S. Bhandari, M.F. Mahon, K.C. Molloy, J. Organometal. Chem. 587 (1999) 101.
[48] J.S. Casas, E.E. Castellano, J. Ellena, M.S. García-Tasende, A. Sánchez, J. Sordo, A. Touceda-Varela, Inorg. Chem. Commun. 7 (2004) 1109.
[49] S.S. Batsanov, Inorg. Mater. 37 (2001) 871.
[50] C.J. Janiak, Chem. Soc., Dalton Trans. (2000) 3885.
[51] J.-A. van der Berg, K.R. Seddon, Cryst. Growth Des. 3 (2003) 643.
[52] G.M. Sheldrick, SHELX 97-2 Users Manual, University of Göttingen, Germany, 1977.
[53] M.C. Burla, M. Camalli, B. Carrozzini, G.L. Cascarano, C. Giacovazzo, G. Polidori, R. Spagna, J. Appl. Cryst. 36 (2003) 1103.
[54] P.W. Betteridge, J.R. Carruthers, R.I. Cooper, C.K. Prout, D.J. Watkinm, J. Appl. Cryst. 36 (2003) 1487.